Design and Development of Lower Divertor for JT-60SA

S. Sakurai, H. Higashijima, H. Kawashima, Y. K. Shibama, T. Hayashi, H. Ozaki,
K. Shimizu, K. Masaki, K. Hoshino, S. Ide, K. Shibanuma, A. Sakasai and JT-60SA team

Japan Atomic Energy Agency (JAEA), Naka, Ibaraki-ken 311-0193, Japan

E-mail contact of main author: sakurai.shinji@jaea.go.jp

Abstract. Lower single null closed divertor with vertical target will be installed at the start of the experiment phase for JT-60 Super Advanced (JT-60SA). Reproducibility of brazed CFC (carbon fibre composite) monoblock targets for a divertor target has been significantly improved by precise control of tolerances and metallization inside CFC blocks. Divertor cassette with fully water cooled plasma facing components and remote handling (RH) system shall be employed to allow long pulse high performance discharges with large neutron yield and they are designed compatible with limited position and size of maintenance ports. Static structural analysis for dead weight, coolant pressure and electromagnetic forces shows that displacement and stress in the divertor module are generally small.

1. Introduction

JT-60SA tokamak project [1,2] has started the construction under both the Japan-EU international program "ITER Broader Approach" and the Japanese domestic program. Phased operation plan is introduced to improve machine performance step by step as shown in Table I. Divertor target will be upgraded according with increase of heating power and the limit of annual neutron yield (Sn) will be increased after establishment of remote handling of plasma facing components. All of plasma facing components shall be actively cooled. Lower single null closed divertor with vertical targets will be installed at the start of "initial research phase". Basic requirements of the lower divertor for JT-60SA [3] are as follows; (1) Handling of 41 MW heating power during 100 seconds, (2) Allowing DEMO relevant plasma shaping factor S = 6~7 and low aspect ratio ~2.5, (3) Compatibility with remote handling maintenance to allow long pulse high performance discharges with large neutron yield.

TABLE I. PHASED OPERATION PLAN OF JT-60SA [3]

Phase		Gas	Sn (/year)	RH	Divertor	Heating power
Initial	I	H	-	R&D	LSN	21.5MWx100s, 23MWx5s
research phase	II	D	4E19		Partial monoblock	21.5MWx100s, 31.5MWx60s, 33MWx5s
Integrated	I	D	4E20	Use	LSN	27MWx100s, 37MWx60s
research phase	II	D	1E21		Full-monoblock	
Extended research phase		D	1.5E21		DN	41MWx100s

2. Design concepts

The objectives of JT-60SA divertor are the support of ITER divertor experiments and the supplement of DEMO divertor design bases. Therefore, JT-60SA divertor has private dome and "V-shaped" corner at the outer divertor to enhance particle recycling and radiation similar to the design concept of ITER divertor. The divertor pumping capability comparable to that in ITER will be implemented to obtain wider particle control range. The divertor geometry of JT-60SA is optimized to allow ITER like plasma configuration and also higher elongation and triangularity plasma which are required for high beta plasma operation in DEMO. The metal wall such as tungsten will be applied for plasma facing components in ITER and DEMO. The

plasma facing material shall be flexibly changed in JT-60SA to investigate physics bases of plasma wall interactions toward DEMO.

In order to satisfy these requirements, the following design concepts are introduced. (A) Carbon armour tiles bolted on water-cooled heatsinks [4] are applied to remove ≤2 MW/m^2 x 100s and transient pulse at 10 MW/m^2 of heat load. Brazed CFC monoblock targets, which can remove 10-15 MW/m^2 of heat flux continuously and can be mass-produced [5], will be installed as vertical divertor targets. (B) Divertor plasma performance of lower divertor geometry with vertical targets for ITER-like plasma configuration had been assessed by using simulation codes. Inner divertor target was moved upward, outer target was moved downward and height of private dome was reduced to increase plasma elongation and triangularity. Height of private dome and size and position of pumping slots were adjusted to keep particle control capability and expected heat flux less than 15 MW/m^2. [6] Divertor plasma performance for expected operational regimes has been confirmed with simulation. [7] Figure 1 shows the dependence of plasma parameters, peak heat flux at the divertor target and particle flux balance at divertor region on the divertor pumping speed S_{pump}. Particle flux balance and peak heat flux at the outer divertor target can be controlled with keeping constant core edge density. In-vessel cryopumps will be installed behind the divertor cassette to obtain enough pumping capability. The divertor pumping speed can be changed by switching on/off of each cryopumps day by day. (C) Divertor cassette integrated with coolant pipe is introduced. Each cassette shall be installed and replaced through a horizontal port of vacuum vessel by remote handling system similar to that for ITER blanket. Figure 2 shows the latest configuration of a lower divertor with a typical plasma configuration. Carbon

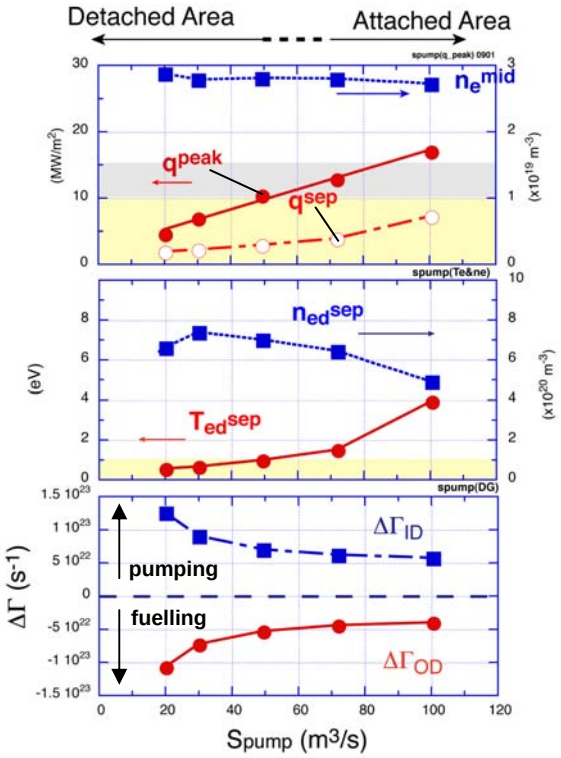

Fig. 1 Controllability of divertor heat flux and particle balance by divertor pumping [7]
q_{peak} is the peak heat flux on the outer target and q_{sep} is the heat flux at the strike point at the outer target. n_{ed}^{sep} and T_{ed}^{sep} are electron density and temperature at the strike point on the outer target, respectively. $\Delta\Gamma_{ID}$ and $\Delta\Gamma_{OD}$ are the net particle flow toward pumping slots at inner and outer divertor, respectively.

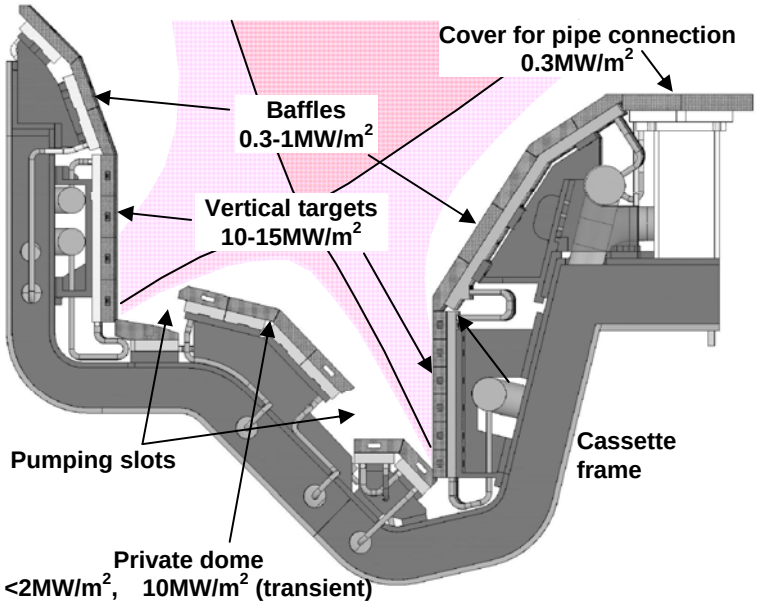

Fig. 2 Latest configuration of lower divertor

armour tiles bolted on water-cooled heatsinks are applied for baffles and private dome, where the maximum steady state heat load including plasma radiation is less than 2 MW/m^2. The CFC monoblock targets will be installed partially for a part of outer targets at the start of "initial research phase" and will replace bolted CFC tiles for inner and outer targets during "initial research phase".

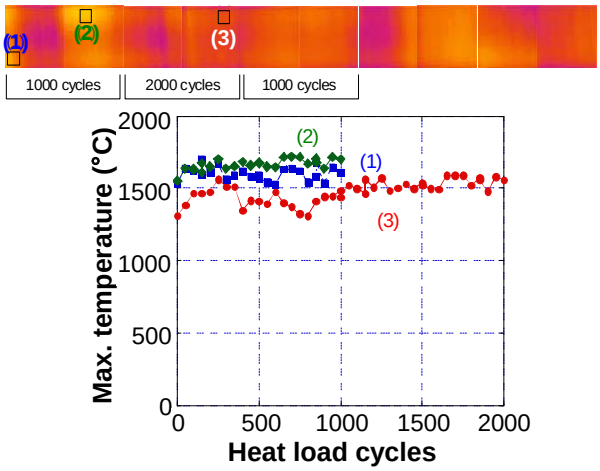

Fig. 3 Thermal images and surface temperature of a mock-up in cyclic heat load test. [5] (1) monoblock with circumferential crack, (2) Maximum temperature in mock-up, (3) typical block with good bonding.

3. CFC monoblock targets

Reproducibility of good bonding has been improved by control of gaps between CFC monoblock/OFHC-Cu buffer layer/CuCrZr cooling tube and metallization inside CFC monoblock. Twelve full-size mock-ups with 10 CFC blocks were manufactured in one furnace. A few CFC block has a radial crack reaching to the surface of CFC block. Circumferential cracks in CFC block near the bonding were also found in 15 blocks of 24 blocks at the edges of each mock-up. These cracks are caused by the difference of thermal expansion between CFC and CuCrZr during brazing. The performance of full-size mock-ups has been tested and confirmed by cyclic heat load test with electron beam irradiation. [5] Surface temperature of CFC blocks has been kept ~1800K after 2000 cycle of ~15 MW/m^2 x 10s even though the CFC monoblock has small circumferential crack as shown in Fig. 3. We assumed criteria of good bonding as 1700°C, which is 200 K higher than ideal surface temperature without crack. Figures 4 shows the total gap between parts shall be 180-195 μm to obtain good bonding performance. The smaller gap makes radial crack in CFC and the larger gap makes wider circumferential cracks which degrade bonding performance. The metallization inside CFC blocks improves bonding but causes scattering of the gap between CFC block and OFCu buffer layer due to scattering of its thickness. Therefore, we are trying other coating methods to improve bonding.

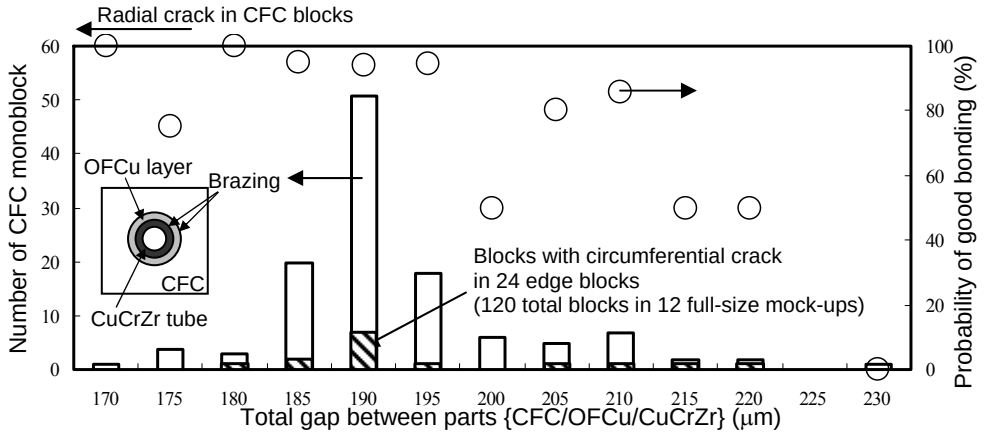

Fig. 4 Relation between tolerance of parts and bonding performance

4. Compatibility with remote handling (RH) maintenance

The key points of design are (i) divertor cassette and RH manipulator for the cassette shall be designed to be a small mechanism to be inserted (and to be deployed) through a horizontal port with 0.66 m width, and (ii) the divertor cassette shall be removed and installed only with access from the plasma side. Only small moving range and torque are required for the manipulator arm in the poloidal direction, because the cassette is located just below the RH rail and can be handed to the transporter at shortest telescopic arm length as shown in Fig. 5. Therefore, driving gear of manipulator is simplified and downsized. Removal procedure of a cassette is summarized in Fig. 6. A part of carbon armour tiles shall be removed by RH manipulator to enable access to fixing bolts of a cassette and coolant pipe connection. Coolant pipe connections located under the top of outer baffle are cut through the access holes between heatsinks by using similar tools for ITER blanket pipe connection. After loosening fixing bolts, a cassette shall be moved 40 mm outward to gain clearance to the inboard first wall. Torque of the downsized manipulator is not enough for moving the cassette weight of 800 kg with a fully expanded telescopic arm. Therefore, a cassette is moved by built-in mechanism. Then, the cassette shall be lifted and transported to the large horizontal port for maintenance by the rail-vehicle system similar to ITER blanket RH system. The cassette can be carried out from the vacuum vessel by the transporter inserted through the horizontal port.

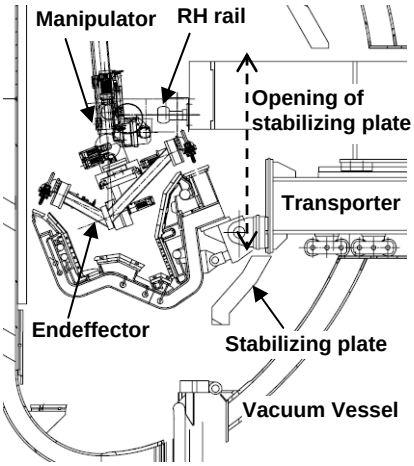

Fig. 5 RH system for divertor cassette [3]

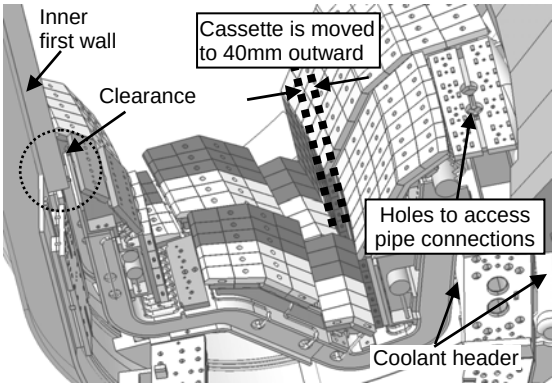

Fig. 6 Removal procedure of a divertor cassette [3]

5. Structural integrity

Two types of disruption were assumed to assess structural integrity. One is major disruption with current quench time of 4 ms (MD 4ms) and the other is vertical displacement event with current quench time of 30 ms (VDE 30ms). Decay and density profile of plasma current and waveform of halo current during disruptions were evaluated with DINA code [8] by assuming toroidal symmetry. [9] Based on the results of DINA code, induced eddy current and its Electromagnetic forces (EMF) were

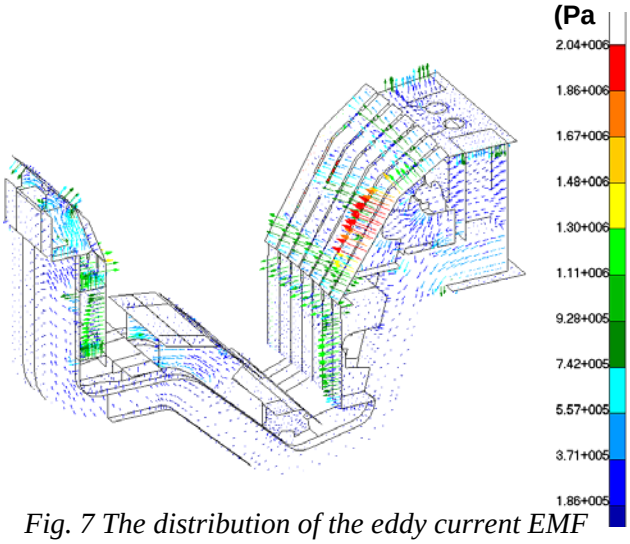

Fig. 7 The distribution of the eddy current EMF at 4.5 ms in MD 4ms case

evaluated by using EDDYCAL [10] code with 10-degree 3-D model of VV, stabilizing baffle plate and a cassette. Halo current EMF was evaluated by assuming halo current flows into top of inner divertor target and flows out at top of outer divertor target for downward vertical displacement event. The maximum value of the evaluated halo current waveform was normalized as (I_{halo}/I_p) x TPF =0.5 (TPF: toroidal peaking factor) by adopting ITER physic bases. Figure 7 shows distribution of the EMF on the cassette at 4.5 ms, when the total EMF on the cassette becomes the maximum, in MD 4ms case. Overturning force due to induced eddy current can be found on inner and outer target and outer baffle.

Figure 8 shows the displacement at 20 ms in VDE 30 ms case evaluated by static structural analysis with finite element model (FEM). The large halo current EMF in the downward direction causes small bending deflection, but overturning force due to eddy current on an outer baffle causes large displacement. Tresca stress of the cassette frame and the local membrane and bending stress near the weld joint of the cassette were assessed. Keys and bolts for fixing heatsinks, support structure and the cassette were modeled by fixing displacement in one direction between the connected nodes of the FEM model. The shear and tensile stresses of the keys and bolts were also evaluated from the reaction force on the nodes. These stresses were confirmed to be within the design criteria for the JT-60SA divertor, which are basically along with the ASME code, except for the support structure and the fixing bolt for the outer baffle. Partial insulating between heatsinks and support structure at the bottom part of outer baffle is found to be useful for reduction of overturning force as shown in Fig. 9. On the contrary, insulation between heatsinks and support induces small eddy current loops and overturning forces in an each heatsink. Structural integrity for the each heatsinks and pipe connections were assessed by the sliced detail model. Figure 10 shows the distribution of membrane and bending stress of the outer vertical target and baffle. The stresses were confirmed to be within design criteria.

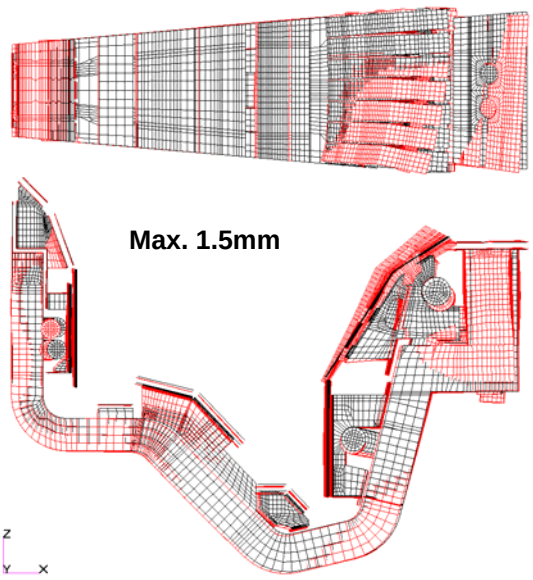

Fig. 8 The displacement of the cassette at 20 ms in VDE 30m case

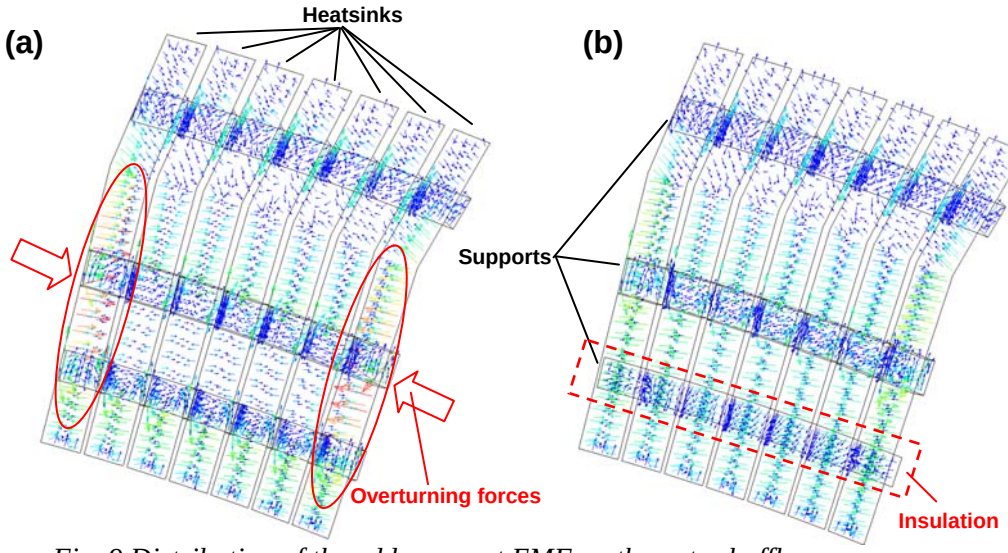

Fig. 9 Distribution of the eddy current EMF on the outer baffle
(a) Fully electrical connection between heatsinks and supports.
(b) Insulation only between heatsinks and the bottom support.

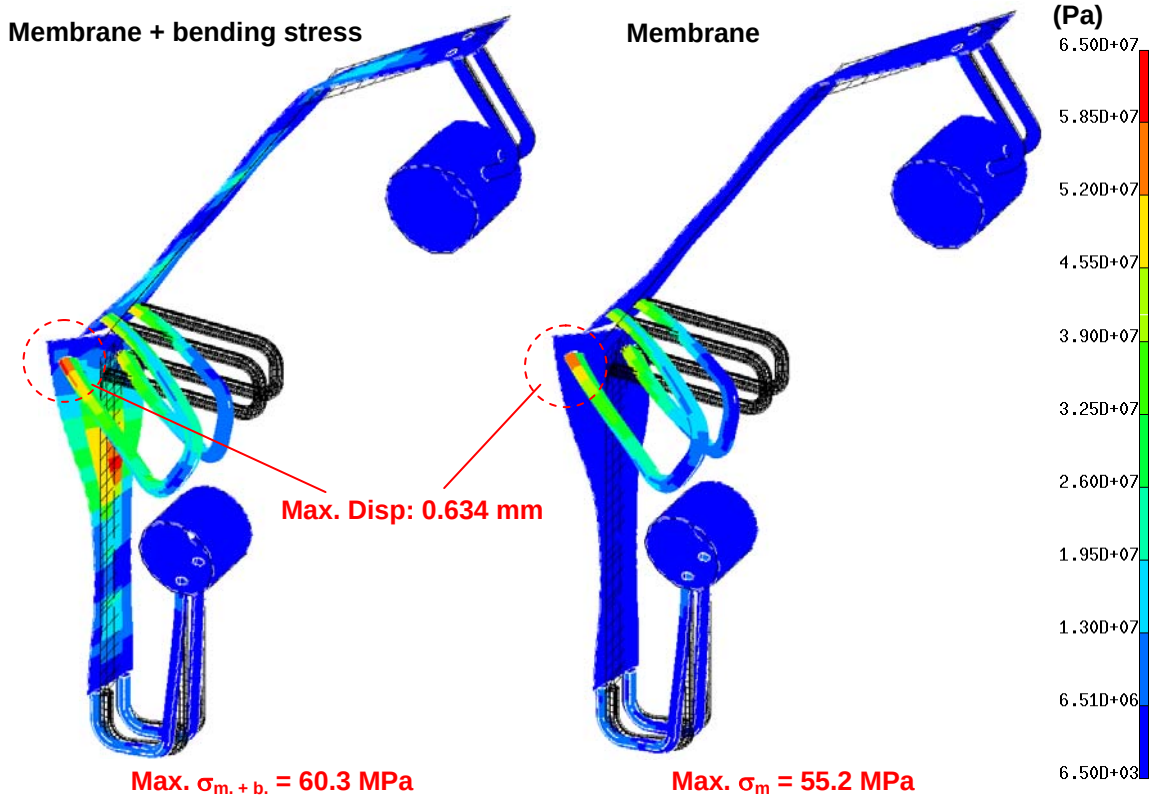

Fig. 10 The displacement and the distribution of membrane and membrane + bending stresses on the outer vertical target and baffle heatsinks and their pipe connections

Acknowledgment

The authors would like to acknowledge Dr. T. N. Todd and Remote handling team in JET for their useful discussion. We also wish to thank Drs. S. Suzuki, K. Ezato and Mr. K. Yokoyama in JAEA for their support in the development and testing of the CFC monoblock target.

Reference

[1] M. Kikuchi, JA-EU satellite tokamak working group and JT-60SA design team, in Proc. of 21st IAEA Fusion Energy Conference, Chengdu, China, IAEA-CN-149/FT/2-5, 2006.
[2] S. Ishida, et al., to be published in Fusion Eng. Des.
[3] S. Sakurai, et al., to be published in Fusion Eng. Des.
[4] K. Masaki, et al., to be published in Fusion Eng. Des.
[5] S. Higashijima, et al., Fusion Eng. Des., **84** (2009) 949.
[6] H. Kawashima, et al., Fusion Eng. Des., **83** (2008) 1643.
[7] H. Kawashima, et al., to be published in J. of Nucl. Mater.
[8] R. R. Khayrutdinov, et al., J. Comp. Phys. **109** (1993) 193.
[9] M. Takechi, et al., this conference.
[10] S. Nishino, et al., IEEE Trans. Magn. **26** (1990) 865.